JCS ePress online publication date 3 August 2010

Decoupling diffusional from dimensional control of signaling in 3D culture reveals a role for myosin in tubulogenesis

Srivatsan Raghavan[1,2], Colette J. Shen[2,*], Ravi A. Desai[2,*], Nathan J. Sniadecki[2], Celeste M. Nelson[1] and Christopher S. Chen[2,‡]

[1]Department of Biomedical Engineering, Johns Hopkins University School of Medicine, Baltimore, MD 21205, USA
[2]Department of Bioengineering, University of Pennsylvania, Philadelphia, PA 19104, USA
*These authors contributed equally to this work
‡Author for correspondence (chrischen@seas.upenn.edu)

Accepted 28 May 2010
Journal of Cell Science 123, 2877-2883

doi:10.1242/jcs.055079

Summary

We present a novel microfabricated platform to culture cells within arrays of micrometer-scale three-dimensional (3D) extracellular matrix scaffolds (microgels). These microscale cultures eliminate diffusion barriers that are intrinsic to traditional 3D culture systems (macrogels) and enable uniform cytokine stimulation of the entire culture population, as well as allow immunolabeling, imaging and population-based biochemical assays across the relatively coplanar microgels. Examining early signaling associated with hepatocyte growth factor (HGF)-mediated scattering and tubulogenesis of MDCK cells revealed that 3D culture modulates cellular responses both through dimensionality and altered stimulation rates. Comparing responses in 2D culture, microgels and macrogels demonstrated that HGF-induced ERK signaling was driven by the dynamics of stimulation and not by whether cells were in a 2D or 3D environment, and that this ERK signaling was equally important for HGF-induced cell scattering on 2D substrates and tubulogenesis in 3D. By contrast, we discovered a specific HGF-induced increase in myosin expression leading to sustained downregulation of myosin activity that occurred only within 3D contexts and was required for 3D tubulogenesis but not 2D scattering. Interestingly, although absent in cells on collagen-coated plates, downregulation of myosin activity also occurred for cells on collagen gels, but was transient and mediated by a combination of myosin dephosphorylation and enhanced myosin expression. Furthermore, upregulating myosin activity via siRNA targeted to a myosin phosphatase did not attenuate scattering in 2D but did inhibit tubulogenesis in 3D. Together, these results demonstrate that cellular responses to soluble cues in 3D culture are regulated by both rates of stimulation and by matrix dimensionality, and highlight the importance of decoupling these effects to identify early signals relevant to cellular function in 3D environments.

Key words: 3D, Signaling, Diffusion, Myosin, Tubulogenesis

Introduction

Cells integrate signals from growth factor stimulation and adhesion to the extracellular matrix (ECM) to regulate many aspects of their function, including gene expression, proliferation, apoptosis and differentiation (Danen et al., 2000; Eliceiri et al., 1998; Schwartz and Ginsberg, 2002). Much of our fundamental understanding of these cooperative intracellular signaling pathways derives from studying cells seeded onto two-dimensional (2D) surfaces coated with ECM proteins. However, many cells in vivo are embedded within a three-dimensional (3D) environment and behave very differently as compared with cells cultured on 2D surfaces (Cukierman et al., 2002). Most cell types removed from their in vivo setting and plated onto tissue culture surfaces quickly lose their differentiated phenotype, take on a more flattened morphology and begin to proliferate (Elsdale and Bard, 1972; Keely et al., 1995; Streuli et al., 1991). By contrast, embedding such cells within ECM scaffolds can often revert these effects, and thereby permits the study of differentiated cell function in vitro within a more physiologically relevant setting (Montesano et al., 1983; Petersen et al., 1992; Streuli et al., 1991). As such, 3D culture has become an increasingly crucial component of many fundamental studies of cell function.

Despite the importance of 3D models, it has been challenging to link 3D-specific cellular behaviors to early signaling events. Cells cultured within 3D matrices are typically embedded within millimeter-scale gels, or 'macrogels', of different ECM compositions including collagens, fibrin and adhesive glycoproteins such as fibronectin and laminin. Numerous studies have demonstrated that diffusion-mediated transport plays a key role in 3D matrices, resulting in spatiotemporal differences in concentrations of soluble stimuli (Griffith and Swartz, 2006; Pluen et al., 1999; Ramanujan et al., 2002). Asynchronous stimulation can obscure detection of early signaling events that drive downstream behaviors. Consequently, whereas differences in cell function are easily observed between 3D and 2D culture, differences in signaling responses have been substantially more difficult to confirm. Here we set out to determine whether distinct behaviors seen in cells cultured within ECM scaffolds are entirely due to the dimensionality of the matrix environment (i.e. 3D vs 2D) or in part from delays in the diffusion of soluble signals to cells.

Results and Discussion

Microgels minimize diffusion barriers to soluble factors

To minimize spatial and temporal gradients due to limitations in the transport of factors through 3D matrices, we scaled down 3D

matrices to micrometer-length scales, such that diffusible factors introduced to the medium would quickly equilibrate inside these 'microgels'. Arrays of 100-μm-deep microwells were used as chambers to form 3D collagen-I-based cell cultures (Fig. 1A,B). Cells within these cultures were morphologically indistinguishable from cells in 2-mm-tall, attached collagen-I gels ('macrogels') (Fig. 1C; supplementary material Fig. S1).

We first confirmed that the experimentally observed transport of soluble factors through the gels could be modeled by diffusive processes (supplementary material Fig. S2A), as has been shown by numerous prior studies (Ramanujan et al., 2002; Van Tomme et al., 2005). We used time-lapse images of fluorescently tagged bovine serum albumin (BSA; molecular mass = 66 kDa) diffusing through collagen-I gels to calculate a diffusion coefficient (supplementary material Fig. S2A), which was consistent with measurements reported by other investigators (Ramanujan et al., 2002; Schuppan et al., 1998). Simulations using this measured diffusion coefficient showed that a 66 kDa protein (the size of a large growth factor) reaches half-maximal concentration at the bottom of macrogels after more than 10 hours, and does not equilibrate until after 72 hours. By contrast, the same protein equilibrates within minutes in microgels (Fig. 1D). Although this effect of delayed equilibration is less pronounced when using molecules of low molecular weight, it is still significant. For example, addition of a solution containing the nuclear dye Hoechst 33342 (molecular mass = 0.616 kDa) to the surface of gels resulted in half-maximal dye accumulation in cells at the base of gels within hours for the several-millimeter-thick macrogels, versus within minutes for 100-μm-thick microgels (supplementary material Fig. S2B). Thus, because of diffusion-dependent delays in the equilibration of soluble factors, cells embedded within macrogels would be stimulated asynchronously by any single soluble factor depending upon the depth of the cell within the gel. Furthermore, mixtures of factors (e.g. serum) would reach cells asynchronously depending upon the diffusion coefficients of each factor in the mixture. These processes severely complicate the interpretation of any measured cellular responses in macroscale 3D settings.

We hypothesized that cells within a macrogel that is exposed to an overlay of medium containing a soluble factor therefore would receive the stimulus at different times depending on their depth within the gel, and that heterogeneous stimulation would be significantly abrogated in microgels. To test this idea, we suspended NIH 3T3 cells within collagen macro- and microgels, stimulated them with TNFα and quantified NFκB translocation to the nucleus for cells near the top versus those near the bottom surface of the gels. By 30 minutes of TNFα exposure, nearly all cells in the microgels were activated, whereas only cells at the top of macrogels were activated (Fig. 1E,F). Cells at the bottom of macrogels showed NFκB nuclear translocation approximately 1 hour after cells at the top, and the rate to reach full activation was halved (supplementary material Fig. S3). Limited soluble stimulation was responsible for the blunted NFκB activation of cells at the bottom of the macrogels, because culturing macrogels on rigid but porous membranes that permitted simultaneous soluble stimulation from the top and bottom robustly activated cells at the bottom of these 'rescue gels' (Fig. 1E,F). Any growth factor binding to collagen-I would further hinder transport through gels, thus accentuating asynchronous soluble stimulation in traditional macrogel culture. Retardations in stimulation onset and rate within macrogels suggest that signaling following soluble factor stimulation is heterogeneous in 3D matrix environments and that diffusion-mediated effects must be accounted for when interpreting signaling responses in 3D cultures.

HGF-induced ERK phosphorylation depends on the rate of stimulation and not on matrix dimensionality

To examine whether diffusion limitations contribute to differential responses between cells cultured on 2D substrates versus in 3D gels, we investigated stimulation of Madin-Darby canine kidney

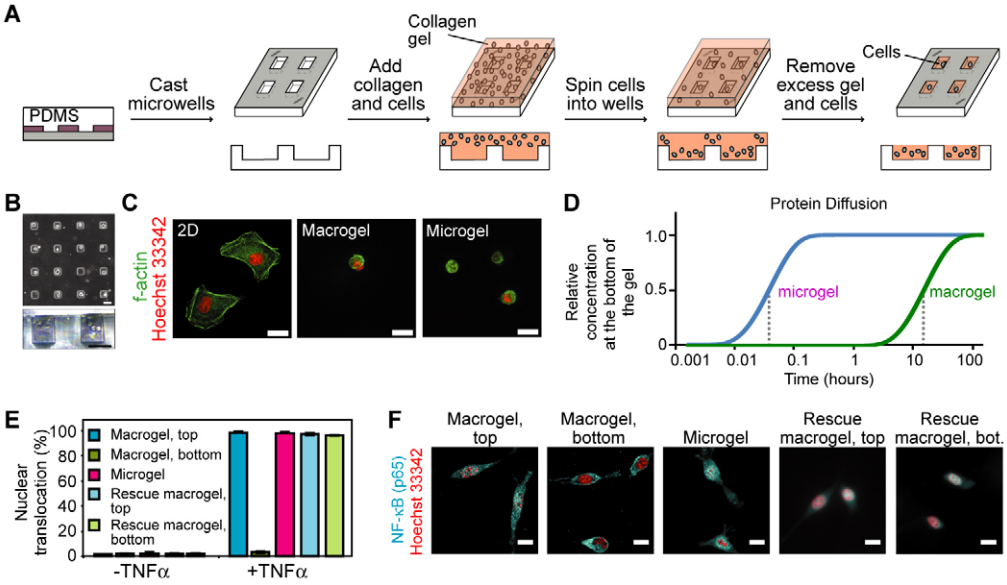

Fig. 1. A microfabricated approach to minimize diffusion barriers in 3D culture. (**A**) Schematic of fabrication of 3D microgels. PDMS, poly(dimethylsiloxane). (**B**) Phase contrast image of individual MCF-10A cells cultured in 42×42×75 μm microgels (top), and a brightfield cross-sectional image of BAMECs suspended within 50×50×60 μm microgels (bottom). Scale bars: 50 μm. (**C**) MDCK cells fixed 24 hours after culture in the indicated matrices. Scale bars: 20 μm. (**D**) Simulations of protein diffusion (molecular mass =66 kDa). Dashed lines indicate time to half-maximal concentration, and correspond to 2.33 minutes for microgels and 15.5 hours for macrogels. (**E**) Quantification of NFκB nuclear translocation in NIH 3T3 cells 30 minutes after stimulation with 25 ng/ml TNFα. Means ± s.e.m. are from three independent experiments. (**F**) NIH 3T3 cells fixed 30 minutes after stimulation with TNFα. Scale bars: 10 μm.

(MDCK) cells by hepatocyte growth factor (HGF), a potent stimulator of migration and tubulogenesis (Montesano et al., 1991; Stoker et al., 1987). Because HGF (65 kDa) has a similar diffusion coefficient to that measured for BSA (66 kDa; supplementary material Fig. S2), our model predicts that HGF would reach the bottom of macrogels extremely slowly (Fig. 1D). Thus, differences in cellular response in macrogels versus on 2D substrates could be attributed in part to altered dynamics of HGF exposure. On 2D surfaces, MDCK cells initially formed cell clusters that scattered upon stimulation with HGF, as expected (Fig. 2A; supplementary material Fig. S4). In 3D macro- and microgels, unstimulated MDCK cells formed multicellular spheroid clusters of comparable sizes. Upon stimulation with HGF, clusters initiated process extension and sprout formation at the tops of macrogels and throughout microgels (Fig. 2A; supplementary material Fig. S5). Interestingly, the sprouting activity of clusters (percentage of clusters forming sprouts, as well as number of sprouts per cluster) decreased with distance from the top surface, and clusters at the bottom of 2-mm-tall macrogels did not respond and formed sprouts even after 72 hours of stimulation, consistent with our prediction of limited diffusion of HGF to the bottom of macrogels. To confirm that this absence of sprouting only at the bottom of gels was owing to limited diffusion of HGF, we stimulated cells in rescue gels simultaneously at the top and bottom of the gel, and observed sprouting in both regions (Fig. 2A; supplementary material Fig. S5). These data highlight the heterogeneous response inherent to macrogels, and argue that there are functional consequences to diffusion-delayed growth factor stimulation.

To assess potential signaling heterogeneities within macrogels, we first examined the dynamics of HGF-induced extracellular related kinase (ERK) activation, which has been associated with scattering and sprouting responses (O'Brien et al., 2004; Potempa and Ridley, 1998). On 2D substrates, HGF induced ERK phosphorylation rapidly and robustly (Fig. 2B; supplementary material Fig. S6). By contrast, cells in macrogels exhibited a muted response to HGF. However, cells within microgels demonstrated a rapid and sustained response that mirrored cells on 2D substrates, suggesting that previously observed ERK activation differences in 2D versus 3D are due to delayed HGF diffusion and not matrix dimensionality (O'Brien et al., 2004; Potempa and Ridley, 1998).

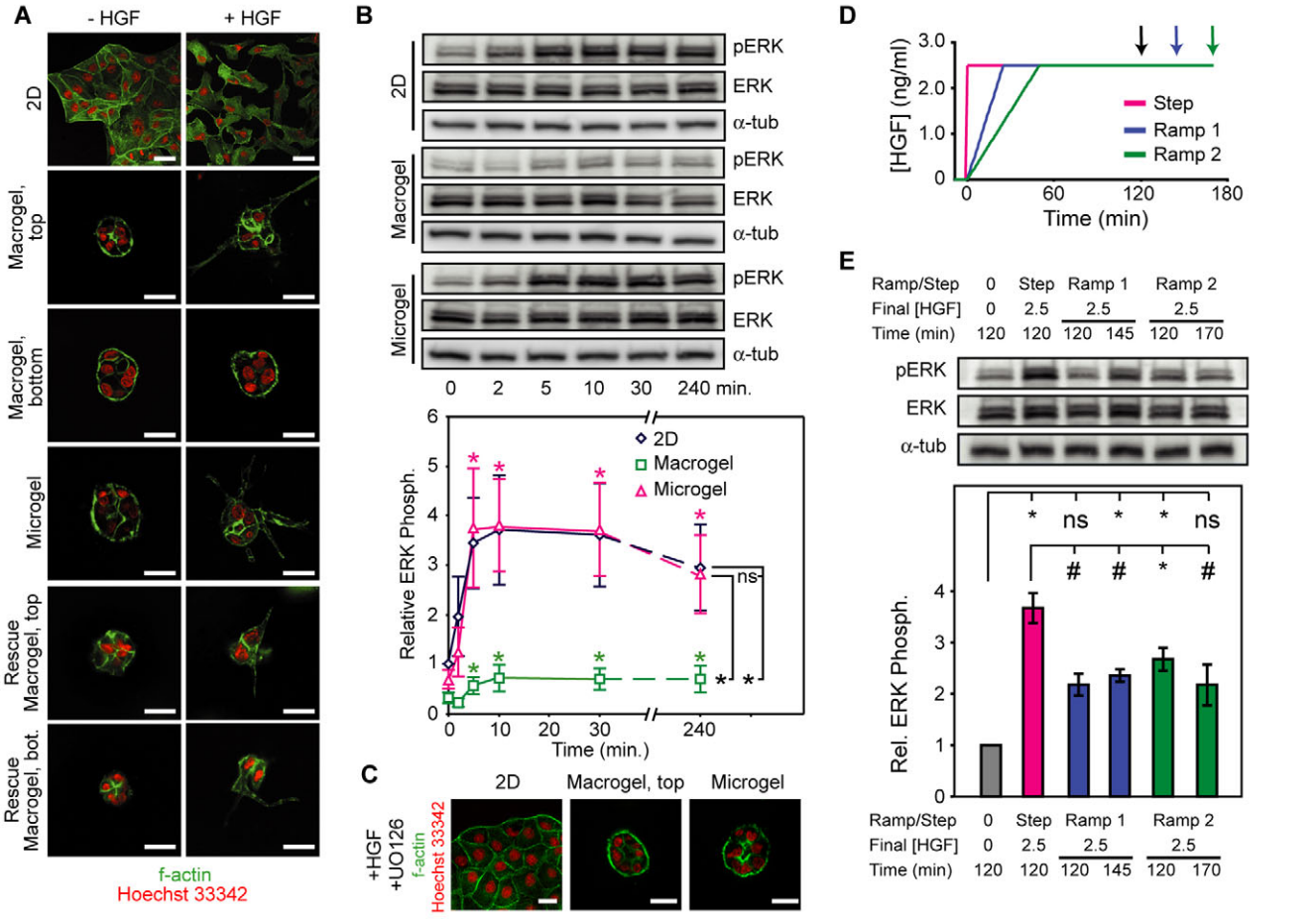

Fig. 2. HGF-induced ERK activation underlying MDCK scattering and tubulogenesis is regulated by rate of stimulation, not matrix dimensionality. (**A**) MDCK cells before and after stimulation with 25 ng/ml HGF for 24 hours. (**B**) ERK phosphorylation in response to 25 ng/ml HGF stimulation in MDCK cells. Means ± s.e.m. are from at least five independent experiments. Colored asterisks in the graph represent $P<0.05$ relative to time 0, via Student's *t*-test with Bonferroni correction for multiple comparisons. Black asterisks represent significantly different ($P<0.05$) profiles between 2D, macrogel and microgel, via Mann-Whitney *U*-test. (**C**) MDCK cells treated with 10 µM U0126 and then stimulated with HGF. (**D**) Profiles of HGF stimulation applied to MDCK cells cultured in microgels. Ramp 1: 0.1 ng/ml/minute; Ramp 2: 0.05 ng/ml/minute. Cells were lysed 2 hours from start or end of stimulation (black, blue, green arrows). (**E**) ERK phosphorylation in response to dynamic stimulation with HGF. Means ± s.e.m. are from at least five independent experiments. *$P<0.05$; #, $P<0.10$, Student's *t*-test with Bonferroni correction for multiple comparisons. Scale bars: 20 µm.

Stimulating rescue gels with HGF from the top and bottom elevated ERK activity compared with macrogels, further implicating diffusion limitations in affecting cell responses in macrogels (supplementary material Fig. S7). MDCK cells stimulated with serum and monitored for activation of a luciferase reporter driven by the serum response element (SRE), a transcription factor downstream of ERK signaling, also responded robustly in microgels and on 2D surfaces, but not in macrogels (supplementary material Fig. S8). Inhibition of ERK signaling with U0126 abrogated MDCK scattering on 2D surfaces and sprouting in gels (Fig. 2C; supplementary material Figs S9, S10), further arguing that ERK signaling has similar importance to migratory events in both contexts. Collectively, these data highlight the challenges of using macrogels to interpret cellular signaling in response to soluble cues.

Cells at the bottom of macrogels might fail to activate ERK simply because the concentration of HGF at the bottom of macrogels never reaches the threshold for ERK activation. Alternatively, it is possible that cells also are sensitive to the rate of stimulation (change in HGF concentration over time), and stimulation rate at the bottoms of gels is substantially slower than at the tops of macrogels or in microgels. Although it is impossible in macrogels to decouple whether rate or only absolute concentrations can affect cellular signaling, using microgels allowed us to directly test whether stimulation rate can impact ERK activation. Specifically, MDCK cells in microgels were exposed to either a step stimulation or two distinct ramp stimulations, all to a final concentration of 2.5 ng/ml HGF (Fig. 2D). Cells responded to the step stimulus with robust ERK phosphorylation, nearly 3.5-fold higher than the unstimulated case (Fig. 2E). This response was muted in both ramp conditions at all assayed time points, demonstrating that the slower stimulation rate dampened the ERK response to HGF. These data reveal a relationship between stimulus rate and cellular response, and suggest that one mechanism by which 3D culture can modulate cellular signaling is by slowing the rates of growth factor stimulation.

HGF-induced MLC activity is determined by matrix dimensionality and regulates tubulogenesis

To determine whether slowed diffusion of HGF can explain other signaling differences in 3D versus 2D culture, we examined other pathways downstream of HGF. Myosin II light chain (MLC) activation by HGF is a key regulator of MDCK cell motility in 2D (de Rooij et al., 2005), but its contribution to morphogenesis in 3D culture is unclear (Ivanov et al., 2008; Kawano et al., 1999; Yu et al., 2003). Stimulation by HGF had little impact on MLC activity (MLC phosphorylation normalized to total MLC) in either cells plated on collagen-coated dishes (2D surfaces) or cells in macrogels (3D), with cells in macrogels exhibiting lower basal activity (Fig. 3A). This comparison suggested either that matrix dimensionality does not significantly modulate MLC phosphorylation in response to HGF, or that diffusion limitations of HGF through collagen gels again confounded the interpretation of biochemical signaling in macrogels. In contrast to macrogels, HGF stimulation of cells in microgels revealed a dramatic suppression of MLC activity; this suppression was largely mediated by an increase in total myosin expression combined with relatively stable MLC phosphorylation. To distinguish between effects arising from differences between collagen coating and collagen gel versus those specifically due to differences between 2D and 3D culture, we examined cells cultured on top of collagen gels. Interestingly, HGF stimulation also induced a decrease in MLC activity in cells on top of gels, similar to that seen in cells within microgels (Fig. 3A). However, this downregulation resulted from a combination of MLC dephosphorylation and enhanced MLC expression, and was transient for cells on the top of gels whereas it was sustained within microgels. These results suggest that myosin activity is impacted by both dimensionality and the nature of collagen presentation (e.g. physisorbed versus gelled), and that the sustained change in MLC signaling observed in microgels is specific to the 3D matrix environment. Furthermore, MLC activity was not significantly altered by different stimulation rates in microgels (supplementary material Fig. S11), suggesting that matrix dimensionality plays a more dominant role than stimulation rate in modulating MLC signaling. Together, these results suggest that certain signals (e.g. ERK) are regulated primarily by stimulation dynamics, whereas others (e.g. MLC) are chiefly regulated by matrix presentation and dimensionality.

To investigate whether the suppression of MLC activity in cells on and in gels discovered here also influences 2D scattering or 3D sprouting, we examined HGF-induced scattering and sprouting of MDCK cells transfected with siRNA against myosin phosphatase target subunit 1 (*MYPT1*) to constitutively enhance myosin activation relative to a transfection control. Transfection with siRNA knocked down MYPT1 and enhanced myosin activity but did not prevent robust scattering on 2D surfaces (both collagen-coated dishes and on top of collagen gels), suggesting a minimal role for the downregulation of MLC activity in 2D scattering (Fig. 3B,C; supplementary material Fig. S12). By contrast, 3D sprouting was inhibited by MYPT1 knockdown, suggesting that the observed HGF-induced downregulation of MLC activity is necessary for sprouting by cells in gels (Fig. 3C; supplementary material Fig. S13). Similarly, treatment with calyculin A, a myosin phosphatase inhibitor that prevents MLC dephosphorylation, did not prevent scattering in 2D, but did inhibit sprouting in 3D (supplementary material Fig. S14). By contrast, HGF-induced scattering and sprouting were not affected by ML-7, a myosin light chain kinase (MLCK) inhibitor (supplementary material Fig. S14), or the ROCK inhibitor Y-27632 (not shown), both of which inhibit myosin phosphorylation. Together, these data demonstrate that myosin activity downregulation, not upregulation, is important specifically for the sprouting response, and illustrate the utility of microgels as a means to identify 3D-specific signaling responses involved in 3D-specific functional events.

Whereas most differences in 2D versus 3D have been attributed to the inherent dimensionality of 3D culture, our studies using microgels demonstrate that some cellular responses are in fact dominated by stimulation rate (e.g. ERK), whereas others are dominated by matrix presentation (gel versus coating) and dimensionality (e.g. MLC). Although rates of stimulation have not previously been considered to be a major player in the effects of 3D environments on cellular signaling and function, this parameter could be important in some settings. For example, recent reports have indicated that the precise concentration of soluble stimuli can localize developmental events at specific times to only a few cells in a specific region (Bollenbach et al., 2008; Manjon et al., 2007; Nelson et al., 2006; Saha and Schaffer, 2006). Although the effect of stimulus rate reported here will ultimately require a more in-depth, quantitative characterization of the basis for this complex and non-linear relationship between binding of the HGF ligand and ERK phosphorylation, these initial studies suggest that stimulus rates can have a functional effect on ERK responses, and therefore

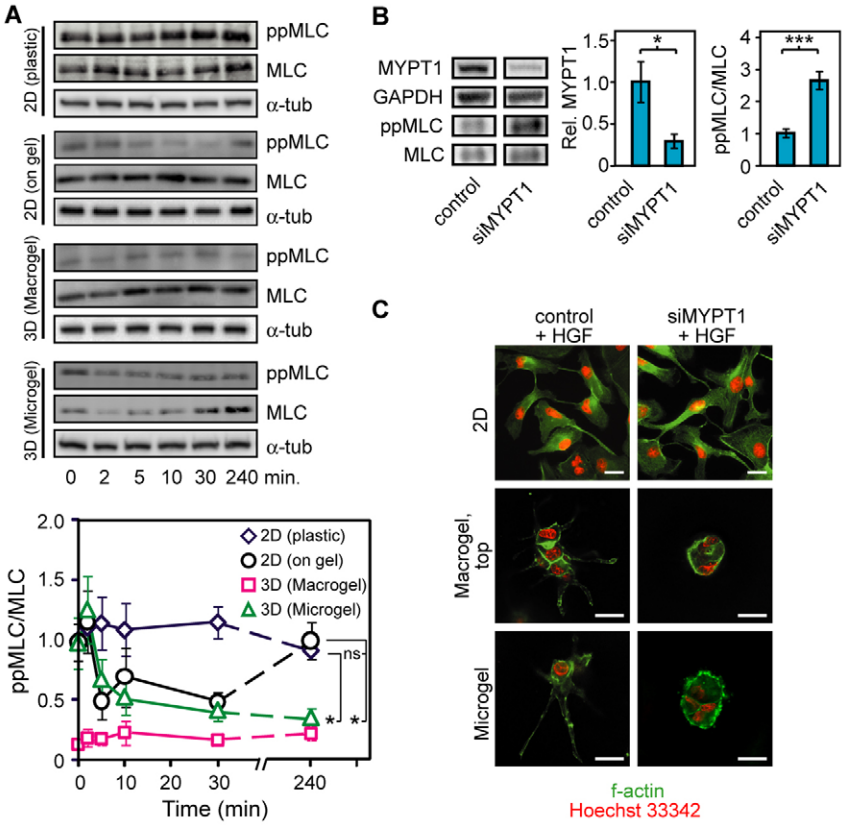

Fig. 3. HGF-induced MLC activity is determined by matrix dimensionality and regulates tubulogenesis. (**A**) Relative MLC phosphorylation in response to 25 ng/ml HGF in MDCK cells. Means ± s.e.m. are from at least five independent experiments. The phosphorylated myosin (ppMLC) blot for macrogels was exposed substantially longer to allow visualization of the relatively weak bands. **P*<0.05 between data points at 240 minutes, via Student's *t*-test with Bonferroni correction for multiple comparisons. (**B**) Protein expression after knockdown of MYPT1 with siRNA relative to a non-transfected control. Means ± s.e.m. are from three independent experiments. **P*<0.05; ****P*<0.005, Student's *t*-test. (**C**) Control or MYPT1-knockdown MDCK cells stimulated with HGF. Scale bars: 20 µm.

illustrate a second mechanism by which to modulate the effect of a diffusible cue.

Using microgels, we also identified an as-yet-unknown HGF-induced downregulation of myosin activity that occurs in 3D microgels, and demonstrated that this downregulation is crucial for tubulogenesis. The ability to directly compare cells on versus within gels revealed that myosin activity in response to HGF can also be downregulated in a 2D setting by contact with a collagen gel. However, this regulation on 2D gel surfaces involves a transient decrease in myosin activity, whereas regulation in 3D contexts seems to sustain downregulated activity by inducing marked myosin expression. Although cell-matrix interactions have previously been shown to regulate both phosphorylation and expression of myosin (Engler et al., 2006), our data suggest a unique contribution of dimensionality to myosin regulation. How dimensionality (embedding of a cell inside a matrix versus placing a cell on top) could exert its effects remains to be determined. One possibility is that engagement of adhesion receptors on all sides (versus one side, as in 2D) might quantitatively increase adhesion signals. However, many functional responses of cells inside gels correlate more closely with limited adhesion contexts. For example, proliferation is often suppressed and differentiation enhanced in 3D cultures (Birgersdotter et al., 2005; Debnath and Brugge, 2005; Petersen et al., 1992; Zegers et al., 2003) and in cultures where adhesion is limited (Chen et al., 1997; Ingber, 1990; Kong et al., 2006). In both of these contexts, cells take on more spherical (less flattened) morphologies, and cell morphology is known to modulate many cellular responses, including myosin activity (Bhadriraju et al., 2007; Chen et al., 1997; McBeath et al., 2004; Meyers et al., 2006). Alternatively, the constrained nature of 3D contexts might allow cellular deposition of matrix-bound factors and autocrine regulation that might not occur in 2D culture (Discher et al., 2009; Lund et al., 2009; Lutolf and Hubbell, 2005). Given these differences, it is not surprising that changes in myosin activity would be regulated by dimensionality and are important during the massive rearrangements required during tubulogenesis. This study provides a starting point to further elucidate how HGF might induce these differential effects in 2D versus 3D environments, and how downregulation of myosin activity might modulate early sprouting events.

We also observed differences in myosin signaling for cells on collagen gels versus cells on physisorbed collagen. Multiple features of collagen gels that are not present in physisorbed collagen, such as collagen ultrastructure (conformation, fibrillar structure, mesh architecture and hydration state) and low mechanical stiffness, could contribute to this effect. Changes in mechanical stiffness have been shown to dramatically affect many cellular functions, such as proliferation (Klein et al., 2009), stem cell differentiation (Engler et al., 2006) and even myosin activity itself (Engler et al., 2006; Paszek et al., 2005). In addition to mechanical stiffness, alteration in collagen ultrastructure can directly impact cellular responses. For example, it has been shown that loss of the fibrillar nature of collagen will reveal cryptic sites in collagen for integrin binding (Xu et al., 2001), and retaining fibrillar structure even when captured onto glass can rescue some cellular responses seen on collagen gels (Elliott et al., 2005). Given these dramatic effects due to matrix mechanics and architecture, comparisons between cells on collagen gel, within collagen gel and on physisorbed collagen will remain important to isolate the effects of stiffness, ultrastructure and dimensionality.

Although macroscale 3D matrices have proven valuable in studying gross cellular phenomena in a 3D context, the inability to uniformly stimulate cells within macrogels and measure their responses has confounded interpretation of signaling responses and identification of early molecular events associated with important cellular behaviors that are unique to 3D settings. Here, we have developed a novel platform to minimize barriers to the diffusion of soluble factors while preserving the 3D context, thus enabling synchronous stimulation of large populations of cells and direct study of cell signaling in 3D culture. Obtaining a clear picture of early dynamic signaling responses, where cells in 2D versus 3D microenvironments are exposed to equivalent stimuli, is a crucial step to begin to delineate the molecular basis for differences between cell behaviors in 2D versus 3D contexts. As such, microgels provide a general platform to study cells in 3D culture within controlled soluble environments, and provide a means to link early signaling events to mechanisms underlying long-term cellular responses.

Materials and Methods

Cell culture

MDCK cells (ATCC) were cultured in high glucose DMEM containing 10% fetal bovine serum (FBS), 2 mM glutamine, 100 U/ml penicillin and 100 μg/ml streptomycin. NIH 3T3 cells (ATCC) were cultured in high glucose DMEM containing 10% bovine serum, 2 mM glutamine, 100 U/ml penicillin and 100 μg/ml streptomycin (all reagents from Invitrogen unless noted). Bovine adrenal microvascular endothelial cells (BAMECs) were obtained from VEC Technologies and were cultured in low-glucose DMEM containing 10% FBS (Hyclone), 10 ng/ml EGF, 3 ng/ml bFGF, 2 mM glutamine, 100 U/ml penicillin and 100 μg/ml streptomycin. MCF-10A cells were obtained from ATCC and were cultured in DMEM:F12 (1:1) supplemented with 5% horse serum, 100 U/ml penicillin, 100 μg/ml streptomycin, 0.02 μg/ml EGF, 0.1 μg/ml cholera toxin, 10 μg/ml insulin and 0.5 μg/ml hydrocortisone (all from Sigma).

Fabrication of microgel constructs and preparation of culture substrates

To generate substrates for microgels, a prepolymer of poly(dimethylsiloxane) (PDMS; Sylgard 184, Dow Corning) was cast onto photolithographically generated master patterns, as previously described (Chen et al., 1997). 2.4 mg/ml liquid neutralized collagen-I (CI; BD Biosciences) was added to the surface of the substrates, and samples were exposed to vacuum to remove air bubbles trapped within wells. 1×10^6 cells/ml in CI was distributed above the wells, and the entire substrate was centrifuged to drive cells into the microwells. Excess collagen and cells were removed by aspiration, followed by gelling at 37°C and addition of medium.

For 2D culture, collagen-coated surfaces were prepared by incubating with a solution of 100 μg/ml CI in 1% acetic acid for 2 hours at room temperature before rinsing and seeding cells. Macrogels were generated by resuspending 1×10^6 cells/ml in CI, pipetting appropriate volumes of CI (for 2 mm height) into culture plates and gelling at 37°C before addition of medium. Rescue gels consisted of macrogels (2 mm height) formed within transwell inserts having rigid but porous membranes permitting diffusion of soluble factors from a reservoir into the bottom of the macrogel (Corning, 8-μm pores). Soluble stimulations were delivered to the top of macrogels and the top and bottom of rescue gels.

Modeling of protein diffusion in collagen gels

A dimensionless form of the 1D diffusion equation:

$$\frac{\partial C_i}{\partial t} = D\frac{\partial^2 C_i}{\partial y^2},$$

where C_i is concentration of solute i, t is time, y is length and D is the diffusion coefficient as determined in supplementary material Fig. S2 of a protein of molecular weight 66 kDa, was used to simulate protein transport through macrogels (2 mm thick) and microgels (100 μm thick). Details regarding model validation are available on request.

Stimulation with growth factors

To monitor NFκB activation, cells were cultured overnight in 0.1% FBS in the specified condition, stimulated with 25 ng/ml TNFα (Roche), and fixed and immunostained with rabbit anti-p65 (clone C-20; Santa Cruz Biotechnology) and Hoechst 33342 (Invitrogen). By mounting macrogel samples between two coverslips, imaging in the appropriate orientation and observing the position of the focal plane digitally during microscopy (with a 40× NA 1.3 objective on an AxioVert 200M; Carl Zeiss), only cells within 100 μm of the top or bottom surface were counted.

For ERK and MLC activation assays, cells were cultured overnight in 0.1% FBS in the specified condition, stimulated with 25 ng/ml HGF (R&D Systems) and lysed. Samples were analyzed for phosphorylated and total ERK and MLC levels by immunoblot [antibodies: mouse anti-ERK, rabbit anti-phospho-ERK and rabbit anti-phospho-MLC (all Cell Signaling); mouse anti-MLC (Sigma)]. For each condition, phospho-protein, total protein and the associated loading control were from the same experiment. Immunoblots were either probed for phospho-protein, stripped and reprobed for total protein (Fig. 3A, 'on gel' and 'macrogel'; supplementary material Figs S6, S7, S9), or phospho-protein and total protein were probed in parallel blots from the same lysate (Fig. 2; Fig. 3A, 'plastic' and 'microgel'; supplementary material Fig. S11). When parallel blots were used, previous data (not shown) confirmed that an equivalent amount of protein was loaded on each blot (s.d.=16%), and as such the loading control was probed from only one of the parallel blots.

For sprouting and scattering assays, cells were seeded in full-serum media in the specified condition for 24-36 hours. Cells were then stimulated with 25 ng/ml HGF for 24-36 hours prior to fixation. U0126 (Calbiochem) was added to the media 1 hour prior to addition of HGF. Lipofectamine RNAiMAX (Invitrogen) was used to transfect MDCK cells with 500 nM siRNA against MYPT1 (custom SMARTpool target sequences: 5′-GATTATTGAGCCAGAGAAA-3′, 5′-CAACTAAACAGGC-CAAATA-3′, 5′-GCAAGACAGTGGCTAAATA-3′ and 5′-GACACAAGATAGT-GACGAA-3′, Dharmacon) 48 hours prior to sprouting stimulation with HGF in gels. For longer duration assays, HGF, inhibitors and media were renewed every 24 hours.

Application of ramp stimuli

Ramped stimuli were applied using a programmable syringe pump (Model 210; KD Scientific) to continuously deliver small doses of concentrated solution containing HGF to the medium overlying cells cultured within microgels. MDCK cells were exposed to either a step stimulation or ramp stimulations (0.1 ng/ml/minute or 0.05 ng/ml/minute), all to final concentrations of 2.5 ng/ml. Cells were lysed 2 hours after either the onset or the completion of stimulation and probed for ERK and MLC via immunoblot with antibodies as above.

Additional details regarding Materials and Methods are available on request.

We thank Rick Assoian, Andre Levchenko, Yangkao Wang, Dana Pirone, Daniel Cohen, Sami Alom Ruiz, Kiran Bhadriraju, Michele Wozniak and Emerson Lim for helpful discussions. This work was supported by grants from the National Institutes of Health (HL73305, EB00262, GM74048), Whitaker Foundation (S.R., C.M.N.), Soros Foundation (C.J.S.), Ruth L. Kirschstein National Research Service Award (N.J.S., C.J.S.), Hartwell Foundation (N.J.S.) and the National Science Foundation (R.A.D.). Deposited in PMC for release after 12 months.

Supplementary material available online at
http://jcs.biologists.org/cgi/content/full/123/17/2877/DC1

References

Bhadriraju, K., Yang, M., Alom Ruiz, S., Pirone, D., Tan, J. and Chen, C. S. (2007). Activation of ROCK by RhoA is regulated by cell adhesion, shape, and cytoskeletal tension. *Exp. Cell Res.* **313**, 3616-3623.

Birgersdotter, A., Sandberg, R. and Ernberg, I. (2005). Gene expression perturbation in vitro-a growing case for three-dimensional (3D) culture systems. *Semin. Cancer Biol.* **15**, 405-412.

Bollenbach, T., Pantazis, P., Kicheva, A., Bokel, C., Gonzalez-Gaitan, M. and Julicher, F. (2008). Precision of the Dpp gradient. *Development* **135**, 1137-1146.

Chen, C. S., Mrksich, M., Huang, S., Whitesides, G. M. and Ingber, D. E. (1997). Geometric control of cell life and death. *Science* **276**, 1425-1428.

Cukierman, E., Pankov, R. and Yamada, K. M. (2002). Cell interactions with three-dimensional matrices. *Curr. Opin. Cell Biol.* **14**, 633-639.

Danen, E. H., Sonneveld, P., Sonnenberg, A. and Yamada, K. M. (2000). Dual stimulation of Ras/mitogen-activated protein kinase and RhoA by cell adhesion to fibronectin supports growth factor-stimulated cell cycle progression. *J. Cell Biol.* **151**, 1413-1422.

Debnath, J. and Brugge, J. S. (2005). Modelling glandular epithelial cancers in three-dimensional cultures. *Nat. Rev. Cancer* **5**, 675-688.

de Rooij, J., Kerstens, A., Danuser, G., Schwartz, M.A. and Waterman-Storer, C. M. (2005). Integrin-dependent actomyosin contraction regulates epithelial cell scattering. *J. Cell Biol.* **171**, 153-164.

Discher, D. E., Mooney, D. J. and Zandstra, P. W. (2009). Growth factors, matrices, and forces combine and control stem cells. *Science* **324**, 1673-1677.

Eliceiri, B. P., Klemke, R., Stromblad, S. and Cheresh, D. A. (1998). Integrin alphavbeta3 requirement for sustained mitogen-activated protein kinase activity during angiogenesis. *J. Cell Biol.* **140**, 1255-1263.

Elliott, J. T., Woodward, J. T., Langenbach, K. J., Tona, A., Jones, P. L. and Plant, A. L. (2005). Vascular smooth muscle cell response on thin films of collagen. *Matrix Biol.* **24**, 489-502.

Elsdale, T. and Bard, J. (1972). Collagen substrata for studies on cell behavior. *J. Cell Biol.* **54**, 626-637.
Engler, A. J., Sen, S., Sweeney, H. L. and Discher, D. E. (2006). Matrix elasticity directs stem cell lineage specification. *Cell* **126**, 677-689.
Griffith, L. G. and Swartz, M. A. (2006). Capturing complex 3D tissue physiology in vitro. *Nat. Rev. Mol. Cell Biol.* **7**, 211-224.
Ingber, D. E. (1990). Fibronectin controls capillary endothelial cell growth by modulating cell shape. *Proc. Natl. Acad. Sci. USA* **87**, 3579-3583.
Ivanov, A. I., Hopkins, A. M., Brown, G. T., Gerner-Smidt, K., Babbin, B. A., Parkos, C. A. and Nusrat, A. (2008). Myosin II regulates the shape of three-dimensional intestinal epithelial cysts. *J. Cell Sci.* **121**, 1803-1814.
Kawano, Y., Fukata, Y., Oshiro, N., Amano, M., Nakamura, T., Ito, M., Matsumura, F., Inagaki, M. and Kaibuchi, K. (1999). Phosphorylation of myosin-binding subunit (MBS) of myosin phosphatase by Rho-kinase in vivo. *J. Cell Biol.* **147**, 1023-1038.
Keely, P. J., Fong, A. M., Zutter, M. M. and Santoro, S. A. (1995). Alteration of collagen-dependent adhesion, motility, and morphogenesis by the expression of antisense alpha 2 integrin mRNA in mammary cells. *J. Cell Sci.* **108**, 595-607.
Klein, E. A., Yin, L., Kothapalli, D., Castagnino, P., Byfield, F. J., Xu, T., Levental, I., Hawthorne, E., Janmey, P. A. and Assoian, R. K. (2009). Cell-cycle control by physiological matrix elasticity and in vivo tissue stiffening. *Curr. Biol.* **19**, 1511-1518.
Kong, H. J., Boontheekul, T. and Mooney, D. J. (2006). Quantifying the relation between adhesion ligand-receptor bond formation and cell phenotype. *Proc. Natl. Acad. Sci. USA* **103**, 18534-18539.
Lund, A. W., Yener, B., Stegemann, J. P. and Plopper, G. E. (2009). The natural and engineered 3D microenvironment as a regulatory cue during stem cell fate determination. *Tissue Eng. Part B Rev.* **15**, 371-380.
Lutolf, M. P. and Hubbell, J. A. (2005). Synthetic biomaterials as instructive extracellular microenvironments for morphogenesis in tissue engineering. *Nat. Biotechnol.* **23**, 47-55.
Manjon, C., Sanchez-Herrero, E. and Suzanne, M. (2007). Sharp boundaries of Dpp signalling trigger local cell death required for Drosophila leg morphogenesis. *Nat. Cell. Biol.* **9**, 57-63.
McBeath, R., Pirone, D. M., Nelson, C. M., Bhadriraju, K. and Chen, C. S. (2004). Cell shape, cytoskeletal tension, and RhoA regulate stem cell lineage commitment. *Dev. Cell* **6**, 483-495.
Meyers, J., Craig, J. and Odde, D. J. (2006). Potential for control of signaling pathways via cell size and shape. *Curr. Biol.* **16**, 1685-1693.
Montesano, R., Orci, L. and Vassalli, P. (1983). In vitro rapid organization of endothelial cells into capillary-like networks is promoted by collagen matrices. *J. Cell Biol.* **97**, 1648-1652.
Montesano, R., Matsumoto, K., Nakamura, T. and Orci, L. (1991). Identification of a fibroblast-derived epithelial morphogen as hepatocyte growth factor. *Cell* **67**, 901-908.
Nelson, C. M., Vanduijn, M. M., Inman, J. L., Fletcher, D. A. and Bissell, M. J. (2006). Tissue geometry determines sites of mammary branching morphogenesis in organotypic cultures. *Science* **314**, 298-300.
O'Brien, L. E., Tang, K., Kats, E. S., Schutz-Geschwender, A., Lipschutz, J. H. and Mostov, K. E. (2004). ERK and MMPs sequentially regulate distinct stages of epithelial tubule development. *Dev. Cell* **7**, 21-32.
Paszek, M. J., Zahir, N., Johnson, K. R., Lakins, J. N., Rozenberg, G. I., Gefen, A., Reinhart-King, C. A., Margulies, S. S., Dembo, M., Boettiger, D. et al. (2005). Tensional homeostasis and the malignant phenotype. *Cancer Cell* **8**, 241-254.
Petersen, O. W., Ronnov-Jessen, L., Howlett, A. R. and Bissell, M. J. (1992). Interaction with basement membrane serves to rapidly distinguish growth and differentiation pattern of normal and malignant human breast epithelial cells. *Proc. Natl. Acad. Sci. USA* **89**, 9064-9068.
Pluen, A., Netti, P. A., Jain, R. K. and Berk, D. A. (1999). Diffusion of macromolecules in agarose gels: comparison of linear and globular configurations. *Biophys. J.* **77**, 542-552.
Potempa, S. and Ridley, A. J. (1998). Activation of both MAP kinase and phosphatidylinositide 3-kinase by Ras is required for hepatocyte growth factor/scatter factor-induced adherens junction disassembly. *Mol. Biol. Cell* **9**, 2185-2200.
Ramanujan, S., Pluen, A., McKee, T. D., Brown, E. B., Boucher, Y. and Jain, R. K. (2002). Diffusion and convection in collagen gels: implications for transport in the tumor interstitium. *Biophys. J.* **83**, 1650-1660.
Saha, K. and Schaffer, D. V. (2006). Signal dynamics in Sonic hedgehog tissue patterning. *Development* **133**, 889-900.
Schuppan, D., Schmid, M., Somasundaram, R., Ackermann, R., Ruehl, M., Nakamura, T. and Riecken, E. O. (1998). Collagens in the liver extracellular matrix bind hepatocyte growth factor. *Gastroenterology* **114**, 139-152.
Schwartz, M. A. and Ginsberg, M. H. (2002). Networks and crosstalk: integrin signalling spreads. *Nat. Cell Biol.* **4**, E65-E68.
Stoker, M., Gherardi, E., Perryman, M. and Gray, J. (1987). Scatter factor is a fibroblast-derived modulator of epithelial cell mobility. *Nature* **327**, 239-242.
Streuli, C. H., Bailey, N. and Bissell, M. J. (1991). Control of mammary epithelial differentiation: basement membrane induces tissue-specific gene expression in the absence of cell-cell interaction and morphological polarity. *J. Cell Biol.* **115**, 1383-1395.
Van Tomme, S. R., De Geest, B. G., Braeckmans, K., De Smedt, S. C., Siepmann, F., Siepmann, J., van Nostrum, C. F. and Hennink, W. E. (2005). Mobility of model proteins in hydrogels composed of oppositely charged dextran microspheres studied by protein release and fluorescence recovery after photobleaching. *J. Control. Release* **110**, 67-78.
Xu, J., Rodriguez, D., Petitclerc, E., Kim, J. J., Hangai, M., Moon, Y. S., Davis, G. E. and Brooks, P. C. (2001). Proteolytic exposure of a cryptic site within collagen type IV is required for angiogenesis and tumor growth in vivo. *J. Cell Biol.* **154**, 1069-1079.
Yu, W., O'Brien, L. E., Wang, F., Bourne, H., Mostov, K. E. and Zegers, M. M. (2003). Hepatocyte growth factor switches orientation of polarity and mode of movement during morphogenesis of multicellular epithelial structures. *Mol. Biol. Cell* **14**, 748-763.
Zegers, M. M., O'Brien, L. E., Yu, W., Datta, A. and Mostov, K. E. (2003). Epithelial polarity and tubulogenesis in vitro. *Trends Cell. Biol.* **13**, 169-176.

Journal of Cell Science